https://doi.org/10.1016/j.apenergy.2018.03.036

Price-responsive model-based optimal demand response control of inverter air conditioners using genetic algorithm*

Maomao Hu[a], Fu Xiao[a, b]

[a] Department of Building Services Engineering, The Hong Kong Polytechnic University, Kowloon, Hong Kong

[b] Research Institute for Sustainable Urban Development, The Hong Kong Polytechnic University, Kowloon, Hong Kong

Abstract

The rapid developments of advanced metering infrastructure and dynamic electricity pricing provide great opportunities for residential electrical appliances, especially air conditioners (ACs), to participate in demand response (DR) programs to reduce peak power consumptions and electricity bills. One of the biggest challenges faced by residential DR participants is the lack of intelligent DR control methods which enable residential ACs to automatically respond to dynamic electricity prices. Most existing studies on DR control of residential ACs focus on single-speed ACs. However, inverter ACs which have higher part-load efficiencies have been extensively installed in today's residential buildings. This paper presents a novel model-based DR control method for residential inverter ACs to automatically and optimally respond to day-ahead electricity prices. A control-oriented room thermal model and steady-state model of inverter ACs are developed and integrated to predict the coupled thermal response of the room and AC for the purpose of model-based control. Optimal scheduling of indoor air temperature set-points is formulated as a nonlinear programming problem which seeks the preferred trade-offs among electricity costs, thermal comfort and peak power reductions. Genetic algorithm (GA) is used to search the optimal solution of the nonlinear programming problem. Simulation results show that compared with the baseline case, the proposed model-based optimal control method can reduce the whole electricity costs and the peak power

* The short version of the paper was presented at ICAE2017, Aug 21-24, Cardiff, UK. This paper is a substantial extension of the short version of the conference paper.

demands during DR hours while meeting thermal comfort constraints. Besides, sensitivity analyses on the trade-off weightings in the optimization objective function demonstrate that electricity costs, occupant comfort and peak power reductions are sensitive to the weightings and the use of the weightings is effective in achieving the best trade-off.

Keywords: Inverter air conditioners; Demand response; Day-ahead electricity prices; Genetic algorithm; Nonlinear programming.

Nomenclature

A	area, m^2
AC	air conditioner
BAS	building automation system
C	electricity price
C	equivalent overall thermal capacitance, J/K
c	specific heat, J/K
DAP	day ahead electricity price
DR	demand response
E	energy consumption during a period
EEV	electronic expansion valve
GA	genetic algorithm
h	specific enthalpy, J/kg
HEMS	home energy management system
HTC	heat transfer coefficient
HVAC	heating, ventilation and air conditioning
J	cost function
K	coefficients of PID controller
MAE	mean absolute error

MAPE	mean absolute percentage errors
N	operating frequency of compressor motor, Hz
NTU	number of transfer unit
P	power consumption, W
P	pressure, Pa
Q	cooling capacity of AC, W
Q	heat gains, W
R	equivalent overall thermal resistance, K/W
RC	resistance-capacitance room thermal model
RMSE	root mean square error
RTP	real-time electricity price
T	temperature, ℃
$\dot{m}$	mass flow rate, kg/s

Greek symbols

α	heat transfer coefficient
α	weighting of thermal comfort
β	weighting of peak power
ε	heat transfer effectiveness
η	compressor efficiency

Subscripts

c	condenser
comp	compressor
e	evaporator
ex	heat exchanger
ext	external surface of wall

i	inlet
in	indoor air
int	internal surface of wall
inter	internal heat gains
is	isentropic process
lb	lower bound
m	internal thermal mass
o	outdoor air/outlet
p	constant-pressure process
r	pressure ratio
ref	refrigerant
set	set-point
solar	heat gain from solar radiation
sur	surface
ty	typical
ub	upper bound
v	constant-volume process
w	wall
win	window

1. Introduction

Power imbalance is a critical issue faced by current electrical grids. The increasing penetrations of intermittent renewable resources, e.g. wind and solar, have made the imbalance situation worse. Buildings are responsible for around 40% of the total energy consumptions worldwide, and consume over 70% of the total electrical energy in the USA [1] and over 90% of the total electricity in Hong Kong [2]. As the major end-user of electricity, buildings have great responsibilities and potentials to

provide peak power reductions during on-peak hours. Since heating, ventilation and air conditioning (HVAC) systems account for a large proportion of the total building electricity use, their power consumptions have direct impacts on power grids [2]. According to California energy demand report, HVAC systems are the major contributors to most of the peak power demands in summer in California [3]. Therefore, demand response (DR) management of building HVAC systems is considered as one of the most promising solutions to grid power imbalance issue in recent years. In commercial buildings, DR technologies such as use of building thermal mass [4, 5] and thermal energy storage systems [6-8] have been adopted to reduce and shift power consumptions of large central HVAC systems. Central HVAC systems are normally managed by advanced building automation systems (BAS) and professional engineers, which enable them to fulfill automatic DR control. Residential ACs, particularly the inverter ACs, are still facing challenges to make automatic DR during on-peak hours.

To fully exploit the DR potentials of residential electrical appliances, advanced metering infrastructure such as smart meter [9] and home energy manage system (HEMS) [10] have been developed and implemented in many residential buildings, which provide great opportunities for residential ACs to make automatic DR. Smart meters enable residential end-users to receive dynamic electricity prices from electric utilities or third-party load aggregators. Two types of dynamic retail electricity pricings are widely used in the USA, i.e. Day Ahead Price (DAP) and Real-Time Price (RTP) [9]. DAP is usually calculated at hourly intervals and announced to the end-consumers one day ahead, while RTP is determined every 5 minutes based on the current electricity supply and demand of grid. In order to reduce electricity costs in the dynamic electricity pricing environment, residential DR participants can reduce the electricity use during high-price periods and shift the electricity use to low-price periods. Automatic DR control methods are essential for residential electrical appliances to respond to dynamic pricing. Smart HEMSs facilitate the implementation of automatic DR control methods and strategies for residential appliances including ACs. Many studies have been conducted on DR control of residential electric appliances in the dynamic pricing environment. The commonly used DR control method for residential ACs is indoor air temperature set-point reset based on the dynamic electricity prices [11-16]. Chen et al. [11] used stochastic optimization and robust optimization approaches to optimize the operation scheduling of six typical residential appliances

based on real-time electricity prices. The objective was to minimize the whole-day electricity payment without largely sacrificing thermal comfort. A mixed-integer linear programming problem was formulated and solved by Hubert et al. [12] to minimize electricity costs. Their work showed that advanced scheduling controllers implemented in HEMS were valuable to fully achieve the DR benefits. Lujano-Rojas et al. [13] proposed an optimal energy management strategy for residential energy system consisting of renewable power generations and electrical vehicles based on real-time electricity prices. The optimized operation scheduling for household appliances and electrical vehicles reduced the electricity bills by 8% to 22% on typical summer days. Thomas et al. [14] developed an intelligent AC controller which can provide the optimal comfort and cost trade-offs for the residents by scheduling the AC on/off status. Li et al. [15] investigated and compared different DR strategies for residential ACs under different dynamic electricity pricings and environmental conditions based on eQUEST simulations. Yoon et al. [16] proposed a price-responsive controller for residential HVAC system which enables to reset temperature set-point when the retail price is higher than the preset price. Simulation results showed that the DR controller can provide up to 10.8% energy cost savings and 24.7% peak power reductions.

Although DR control methods of residential AC have been extensively studied, the ACs considered in previous work were all single-speed ACs which only allowed on-off control. The on-off controlled ACs have a big disadvantage of undesired current peaks during state transitions [17]. The single-speed ACs are also gradually replaced by inverter ACs which have gained an increasing market share in recent years due to its higher efficiency under part-load conditions [18]. A major difference between single-speed and inverter ACs is the performances of the latter depend on not only the indoor and outdoor environmental conditions, but also the operating frequencies of the compressor motor. Therefore, the energy performance models of AC in previous residential DR research are not applicable for DR study of inverter AC. In addition, conventional local control methods for inverter AC such as PID control, fuzzy logic control and artificial neural network, are incompetent to address the DR optimization problems with multiple objectives and involving multiple variables such as weather conditions, occupancy and dynamic electricity pricing [19, 20]. Model-based optimal control method, as an advanced control approach, can simultaneously take account of all influential variables

in a real process using model-based prediction techniques and optimally control the dynamic system by solving optimization problems.

To bridge the research gaps, the present paper aims to develop a model-based optimal DR control method for inverter ACs to achieve electricity cost savings and peak power reductions in the dynamic electricity pricing environment without sacrificing residents' thermal comfort. Specifically, three major contributions are made in the present study. First, a steady-state physical model for inverter ACs is developed using the component-wise modeling techniques. Steady-state performance data (cooling capacity and coefficient of performance, COP) of inverter ACs under various environmental conditions and operating frequencies can be determined using the steady-state physical model. Second, the inverter AC model is integrated with a resistance-capacitance (RC) room thermal model which was developed and validated in our previous work [21]. A PID feedback controller is adopted to adjust the operating frequency of the variable-speed compressor motor to regulate the indoor air temperature. The integrated model is used to predict the future system performances under changing operating conditions. This is a big improvement on most previous building DR research, in which the performance of AC was predicted using simple regression equations rather than more realistic performance prediction. Third, we formulate and solve the model-based compound optimization problem by adopting the weighted sum approach to realize automatic DR from residential inverter ACs. The user-definable weightings in the compound objective function enable DR participants to choose their preferred trade-offs among electricity costs, thermal comfort and peak power reductions. GA, as an advance and effective optimization solver, is used to search the optimal scheduling of indoor air temperature set-points for AC local PID controller in the day-ahead electricity pricing environment.

The rest of the paper is organized as follows. In Section 2, we develop and identify a room thermal model and steady-state model of an inverter AC and integrate them. In Section 3, the framework of the model-based DR control method for inverter ACs is introduced. In Section 4, we compare the performance of the model-based optimal DR control method with that of the baseline case based on simulation tests, in terms of electricity cost, peak power reduction and indoor air temperature

deviation. Besides, sensitivity analyses are carried out to investigate the impacts of the weightings on optimization results. Finally, the conclusions are presented in Section 5.

2. Development of integrated thermal response models of room and inverter AC

2.1. Room thermal model

2.1.1. Room model development

Building models used in popular building simulation tools such as TRNSYS, EnergyPlus and eQUEST are not suitable for the development of model-based control methods since the complex building models are usually not computationally efficient. In our previous study [21, 22], we have developed, identified and validated a grey-box resistance-capacitance (RC) room thermal model as illustrated in Fig. 1. The RC model is a grey-box room thermal model which can be trained using the collected data from smart in-home sensors. With the simple structure, the RC model can be easily implemented in the model-based controller to predict the room thermal dynamics. The energy balance for the external/internal walls, indoor air and internal thermal mass are given by Eqs. (1) - (4).

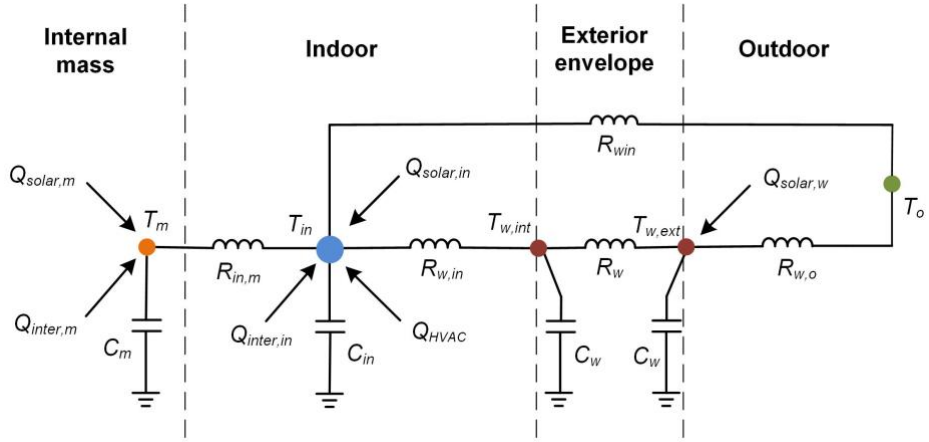

Fig. 1. Schematic of the grey-box thermal model of residential buildings.

$$C_w \frac{dT_{w,ext}}{dt} = \frac{T_o - T_{w,ext}}{R_{w,o}} + \frac{T_{w,int} - T_{w,ext}}{R_w} + Q_{solar,w} \quad (1)$$

$$C_w \frac{dT_{w,int}}{dt} = \frac{T_{w,ext} - T_{w,int}}{R_w} + \frac{T_{in} - T_{w,int}}{R_{w,i}} \quad (2)$$

$$C_{in} \frac{dT_{in}}{dt} = \frac{T_m - T_{in}}{R_{in,m}} + \frac{T_{w,int} - T_{in}}{R_{w,in}} + \frac{T_o - T_{in}}{R_{win}} + Q_{solar,in} + Q_{inter,in} + Q_{HVAC} \quad (3)$$

$$C_m \frac{dT_m}{dt} = \frac{T_{in} - T_m}{R_{in,m}} + Q_{solar,m} + Q_{inter,m} \quad (4)$$

where R and C represent the heat resistance and capacitance, respectively; T denotes temperature; subscripts *in, o, w, int, ext, win* and *m* indicate indoor air, outdoor air, exterior wall, internal wall surface, external wall surface, window and internal mass, respectively; $Q_{solar,w}$, $Q_{solar,in}$ and $Q_{solar,m}$ are solar heat gains absorbed by external wall surface, indoor air and internal mass, respectively; $Q_{inter,in}$ and $Q_{inter,m}$ are internal heat gains absorbed by indoor air and internal mass, respectively. Detailed methods for determining Q_{solar} and Q_{inter} and the model identification algorithm can be found in our previous work [23].

2.1.2. Room model parameter identification

A residential building (L×W×H: 4.8m×3.6m×3m) in Hong Kong was chosen to test the RC room thermal model in this study. The window-wall-ratio of the exterior wall (3.6m×3m) is 0.2. A smart sensor was installed in the room to collect the data of indoor air temperature at 10-minute intervals. A five-day measurement of indoor air temperature from the smart in-home sensor was used to identify the unknown parameters in the room model. The identification results are: C_w = 2,220,800 J/K, C_{in} = 225,440 J/K, C_m = 30,585,600 J/K, R_{win} = 0.0450 K/W, R_w = 0.0478 K/W, $R_{w,o}$ = 0.0023 K/W, $R_{w,in}$ = 0.0074 K/W, $R_{in,m}$ = 0.0009 K/W. The next five-day indoor air temperatures were used to validate the model. Fig. 2 shows the sampled and modeled data of the indoor air temperature during the model training and validation sessions. The results show that the room thermal model is able to predict the indoor air temperature in a relatively high degree of accuracy.

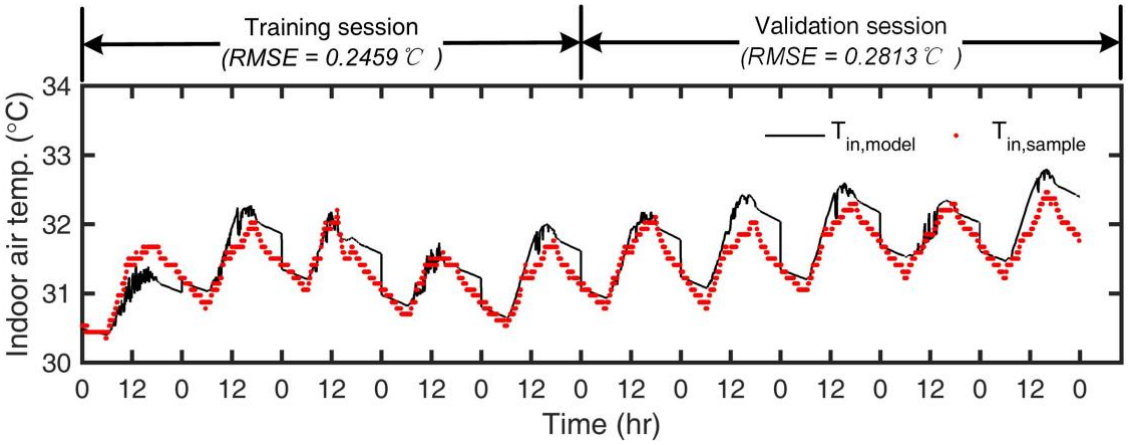

Fig. 2. Modeled and sampled indoor air temperature profiles during the training and validation sessions.

2.2. Steady-state physical model of inverter ACs

2.2.1. AC model development

AC model can be generally classified into transient model and steady-state model. The refrigerant dynamics in residential AC are much quicker than the thermal dynamics of room. The refrigerant re-distributions in different AC components normally accomplish in a short period, around 100 seconds [24, 25]. Therefore, a steady-state AC model is developed to predict the coupled dynamic behaviors of room and AC under time-varying internal and external conditions. Steady-state performances of inverter AC (cooling capacity Q and coefficient of performance COP) are different under different operating conditions including different compressor frequencies N_{comp} as well as different indoor and outdoor air temperatures, i.e. T_{out} and T_{in}. Since AC manufacturers seldom provide enough performance data in the full range of operating conditions, the physical modeling method is developed in this study to predict the performances of typical ductless split inverter AC. For simplification in control application, only four major components including condenser, evaporator, variable speed compressor and electronic expansion valve are modeled in this paper. Other minor components such as accumulator, refrigerant pipeline, sub-cooler and receiver are not considered here.

Variable-speed compressor

Refrigerant mass flow rate and enthalpy at the compressor outlet are the key outputs of the compressor module. The refrigerant mass flow rate through the compressor and the refrigerant enthalpy at the compressor outlet are given by Eqs. (5) - (6), respectively.

$$\dot{m}_{comp} = N_{comp} V_{comp} \rho_{comp} \eta_v \tag{5}$$

$$h_{comp,o} = h_{comp,i} + (h_{comp,o,is} - h_{comp,i})/\eta_{is} \tag{6}$$

where N_{comp}, V_{comp}, ρ_{comp} are the rotational speed of compressor motor in Hz, effective displacement volume, and refrigerant density at the inlet, respectively; $h_{comp,i}$, $h_{comp,o}$ are the enthalpies at the compressor inlet and outlet; $h_{comp,o,is}$ is the enthalpy at the compressor outlet under an isentropic compression; η_v and η_{is} are compressor volumetric efficiency [26, 27] and isentropic efficiency [25, 28, 29] which can be approximately calculated by Eqs. (7) - (8), respectively.

$$\eta_v = 1 + c_{comp} - c_{comp}(P_{comp,o}/P_{comp,i})^{c_v/c_p} \tag{7}$$

$$\eta_{is} = c_0 + c_1 N_{comp} + c_2 N_{comp}^2 + c_3 P_r + c_4 P_r^2 \quad (8)$$

where $P_{comp,o}$ and $P_{comp,i}$ are the refrigerant pressures at the compressor outlet and inlet, respectively; P_r is the ratio of compressor outlet pressure to the inlet pressure; c_{comp} is the compressor clearance ratio; c_v and c_p are the constant volume and constant pressure specific heats at the compressor inlet, respectively; c_0- c_4 are coefficients which can be empirically identified from the actual compressor.

Electronic expansion valve

Expansion devices are used in the refrigeration systems to regulate the refrigerant mass flow rate into the evaporator and maintain the refrigerant superheat at the evaporator outlet. In recent years, due to its superior performance in control, electronic expansion valves (EEV) have been implemented in inverter AC or heat pump to control the cooling capacity and superheat instead of the conventional expansion devices such as capillary tubes and thermostatic expansion valves [30]. Refrigerant mass flow rate through an EEV can be modeled using Eq. (9). Since refrigerant expansion process in EEV can be considered as being adiabatic, the enthalpy at the EEV outlet therefore can be given by Eq. (10).

$$\dot{m}_v = C_v A_v \sqrt{\rho_v (P_c - P_e)} \quad (9)$$

$$h_{v,o} = h_{v,i} \quad (10)$$

where C_v, A_v, ρ_v are the orifice coefficient, valve opening area, refrigerant density, respectively; P_c and P_e are refrigerant pressures at the condenser and evaporator, respectively; $h_{v,o}$ and $h_{v,i}$ are the refrigerant enthalpies at the EEV inlet and outlet, respectively.

Heat exchangers

Heat exchangers, including condenser and evaporator, are responsible for conducting the heat transfer between refrigeration system and surroundings. Based on the fundamental principles of mass, momentum and energy conservations, the dynamics of the two-phase flow in heat exchangers can be represented by a set of elaborated, nonlinear partial differential equations [28]. The heat exchangers are assumed to be one-dimensional, and the pressure drops are assumed to be negligible. The moving boundary approach is widely adopted for both transient modeling [24, 25, 31-33] and steady-state modeling [29, 34] of heat exchangers. The method is able to capture the characteristics of multiple

fluid phase heat exchangers while preserving the simplicity of lumped parameter models. The condenser is normally divided into three zones based on the refrigerant state, i.e. de-superheated, two-phase, and subcooled zones, and the evaporator is divided into two zones, i.e. two-phase and superheated zones. With these assumptions, the one-dimensional steady-state model of each zone can be represented by the conservation equations of mass and energy, which only contain the derivatives to the length of the zones. After integration along the length, the steady state model of a heat exchanger zone can then be transformed into the two algebraic equations as follows:

$$\dot{m}_{ex,o} = \dot{m}_{ex,i} \tag{11}$$

$$h_{ex,o} = h_{ex,i} + Q_{ref,air}/\dot{m}_{ex,i} \tag{12}$$

where $\dot{m}_{ex,i}$ and $\dot{m}_{ex,o}$ are the mass flow rates at the inlet and outlet of the zone, respectively; $h_{ex,i}$ and $h_{ex,o}$ are the enthalpy at the inlet and outlet of the zone, respectively; $Q_{ref,air}$ is the heat exchanged between the refrigerant and the air in that zone (negative value for the condenser). The heat transfer rates $Q_{ref,air}$ in heat exchangers are calculated by effectiveness-number of transfer units (ε-NTU) method. The details of ε-NTU method and heat transfer correlations can be found in Appendix A.

2.2.2. AC model identification and validation

There have been a number of experimental studies of steady-state performances of residential ACs [35-37]. Gayeski [37] carried out quite elaborate experiments for a Mitsubishi split-type inverter AC with a rated cooling capacity of 2.5kW. It is one of the most popular types of residential inverter ACs and the main specifications are listed in Table 1. However, the experimental results in [37] did not contain the complete performance data. For comparison convenience, the same split-type inverter air conditioner was chosen for physical modeling under a wide range of typical operating conditions. The typical operating conditions are the combinations of different compressor rotational speeds, indoor air temperatures and outdoor air temperatures, i.e. N_{ty} = [20, 30, … , 100], $T_{out,ty}$ = [23, 26, 29, 32, 35, 38], $T_{in,ty}$ = [21, 24, 27, 30, 33, 36].

Table 1. Main specifications of the inverter AC

Item		Specification
Refrigeration		R410A
Compressor	type	rotary piston type
	piston displacement volume (cm^3)	10
EEV	type	step motor
	inner diameter (mm)	4
Evaporator	dimension (L×W×H) (m)	0.62×0.03×0.34
	row number	2
	loop number	2
	tube number per row	16
	tube length per row (m)	0.62
	tube outer diameter (mm)	6.8
	tube inner diameter (mm)	5.2
	fin number	488
	fin pitch (mm)	1.17
	fin thickness (mm)	0.102
Condenser	dimension (L×W×H) (m)	0.86×0.5×0.022
	row number	1
	loop number	2
	tube number per row	12
	tube length per row (m)	0.86
	tube outer diameter (mm)	6.5
	tube inner diameter (mm)	4.9
	fin number	610
	fin pitch (mm)	1.34
	fin thickness (mm)	0.0762

To validate the model, 40 sets of experimental data by Gayeski [37] are compared with the modeled data under the same operating conditions. Among the compared data, the ranges of indoor air temperature, outdoor air temperature and compressor speed are 23-38 ℃, 24-36 ℃, and 19-95 Hz, respectively. Fig. 3 shows the comparisons between the modeled data and the experimental data. The deviations are mainly in the range of ±15%. The mean absolute percentage errors (MAPEs) between the predicted and tested cooling capacity and COP are 5.56% and 11.94%, respectively.

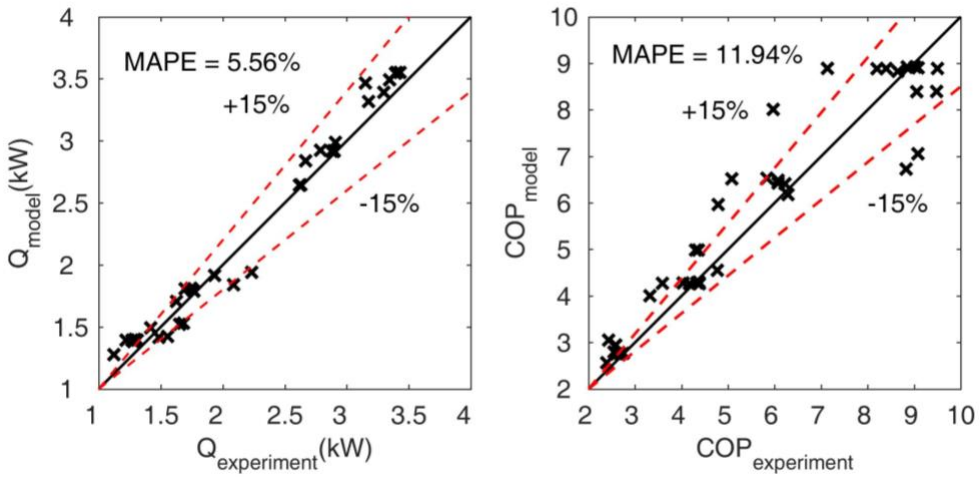

Fig. 3. Comparisons between the modeled data and experimental data of the inverter AC.

Fig. 4 shows the performances of the inverter AC at the compressor speeds of 30Hz, 60Hz and 90Hz predicted by the model. The cooling capacity and COP of the inverter AC mainly depend on the compressor speed. The cooling capacity increases with the increase of compressor speed, but the COP decreases with the increase of compressor speed. The cooling capacity increases with the increase of indoor air temperature and decreases with the increase of outdoor air temperature. Compared to indoor air temperature, outdoor air temperature has a larger effect on COP. The trends predicted by the steady-state model are reasonable and typical for variable-speed ACs, therefore, the steady-state model does not suffer from the overfitting issue and can predict the change of performance with the operating conditions correctly.

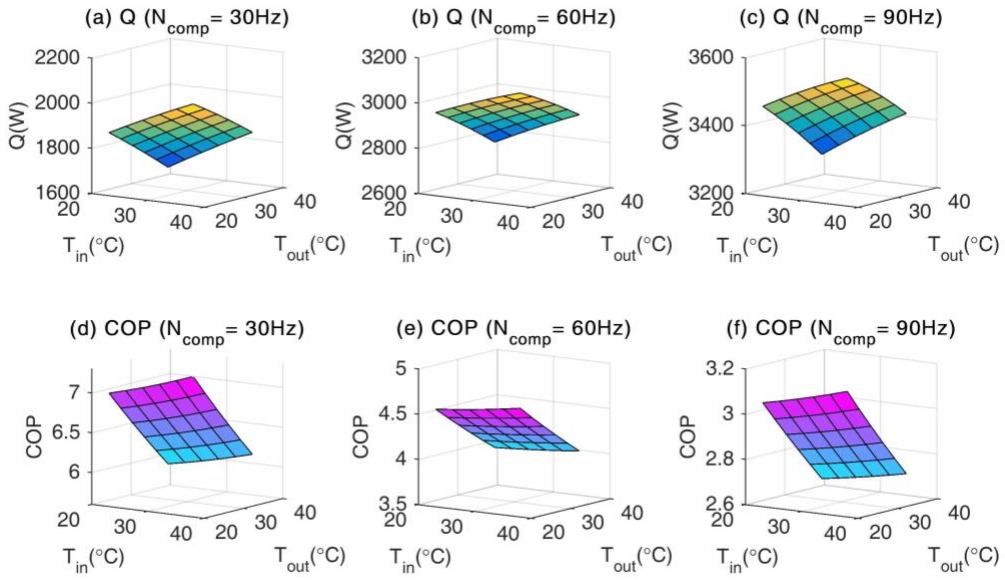

Fig. 4. Performances of the inverter AC at the compressor speeds of 30Hz, 60Hz and 90Hz, respectively.

2.3. Integration of thermal response models

A room temperature controller plays the function of connecting the room thermal dynamics with the inverter AC. The inverter AC controller in the present study is designed using a PID control structure. Fig. 5 depicts the block diagram of the integrated thermal response models and frequency-based control method of inverter AC. After detecting the temperature difference from the set-point, the PID controller computes and outputs the actuating signal of rotational speed to the inverter compressor motor. Under the specific compressor rotational speed and weather disturbances, the cooling capacity and COP of inverter AC can be determined using the developed AC model. The inverter AC then delivers the cooling capacity into the air-conditioned room removing the heat gains caused by the disturbances including outdoor air temperature, solar radiation, and internal heat gains.

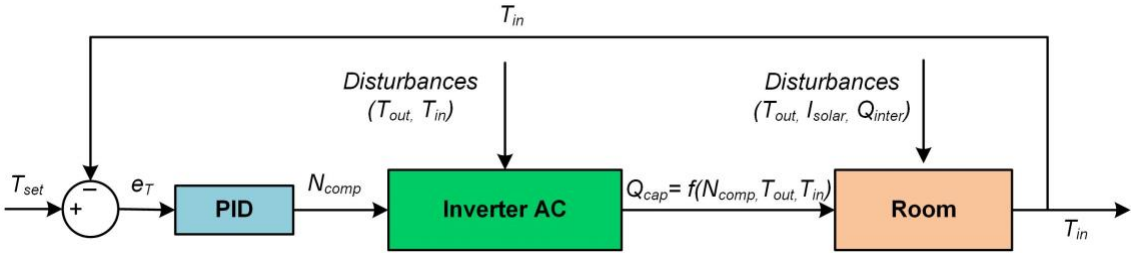

Fig. 5. Block diagram of the integrated thermal response models and frequency-based control method of inverter AC.

3. Model-based demand response control method for inverter ACs

3.1. Outline of the model-based control method

The basic idea of the model-based optimal control is to use the integrated model to predict the performances of inverter AC based on the predictions of weather conditions, occupancy and day-ahead electricity prices. GA is used to search the optimal control signal, i.e. indoor air temperature set-point schedule.

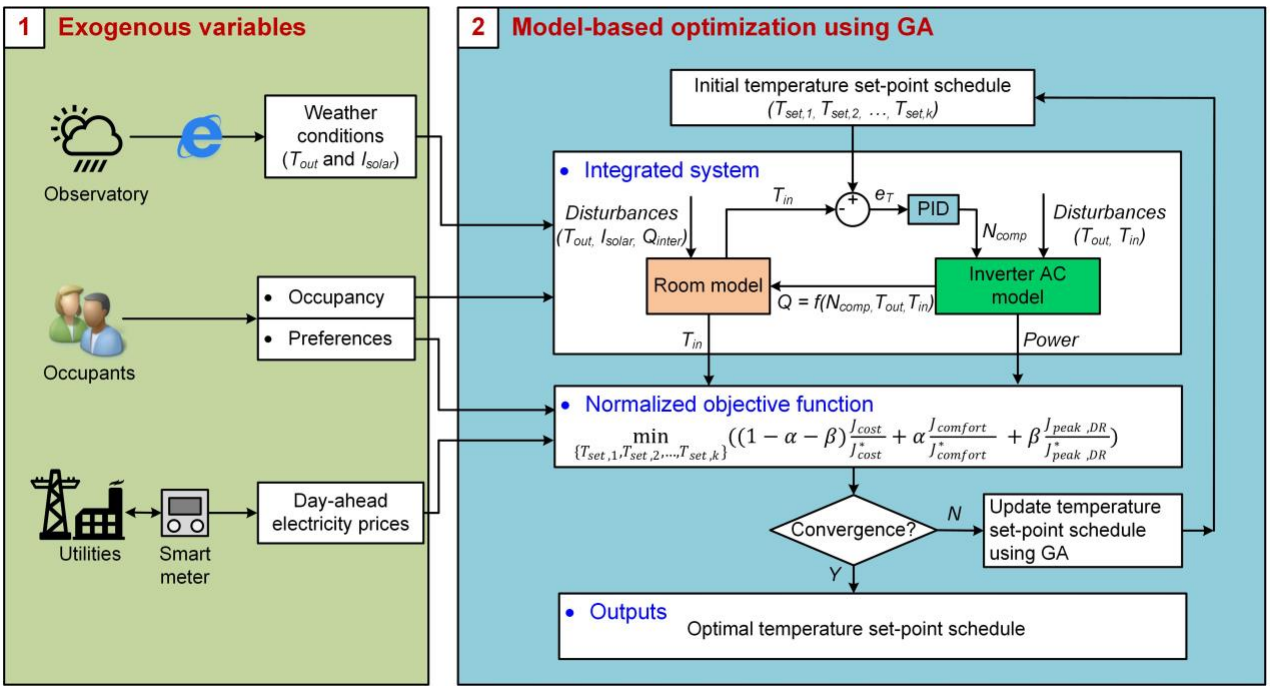

Fig. 6. Framework of the model-based optimal load control methodology of inverter ACs.

As shown in Fig. 6, the whole process of the model-based optimal DR control of inverter AC includes two major steps: preparation/prediction of exogenous input variables and model-based optimization using the GA solver. Weather conditions including outdoor air temperature and solar radiation are required for the predictions of the room thermal dynamics and AC performance, which may come from local observatory or from prediction models [38]. The presence of occupant will influence the room thermal response and hence it is an influential variable in the room thermal model. With the aid of advanced infra-red sensing technology, the presence of occupant can be determined conveniently. However, considering the number of residents in a room is small and more or less the same, it can be pre-defined. Dynamic electricity prices are available from smart meters. The integrated thermal response models of an air-conditioned room and an inverter AC are used to predict the AC power

consumption and indoor air temperature with the inputs. In the end, an optimization problem is formulated and solved using GA to find the day-ahead optimal schedule of indoor air temperature set-point.

3.2. Optimization problem formulation

The optimization problem in this study is a multi-objective optimization problem, which includes three objectives, i.e. minimization the total electricity cost (J_{cost} as defined by Eq. (13-a)), the thermal comfort deviation ($J_{comfort}$, as defined by Eq. (13-b)) considering home residents and minimization of the peak power demand during DR hours ($J_{peak,DR}$, as defined by Eq. (13-c)) considering the power grids. The total electricity cost (J_{cost}) is the sum of the products of the hourly energy consumption of inverter AC (E_i) and the hourly electricity price (C_i). The total comfort deviation ($J_{comfort}$) is the root mean square error of the indoor air temperatures to the temperature set-points. The peak power demand ($J_{peak,DR}$) is the maximum power consumption of the inverter AC during DR hours. The time steps of energy consumption (E_i) and electricity price (C_i) are 1 hour and the time intervals of the indoor air temperature ($T_{in,j}$) and the power consumption (P_l) are both 1 minute. The optimization processes of each objective function are subject to the comfort constraint, Eq. (14), which limits the temperature set-point between a lower bound ($T_{set,lb}$) and an upper bound ($T_{set,ub}$). The three objectives, i.e. Eqs. (13-a) - (13-c), are not independent but conflicting. For example, when minimizing the thermal comfort deviation, it may result in the increase of the electricity cost and the increase of the peak power demand. When minimizing the peak power demand, the deviation of thermal comfort may increase.

The methods of multi-objective optimization problem can be divided into classical methods and evolutionary methods. Classical methods include the weighted sum method, epsilon constraint method, weighted metric method, value function method and so on. Evolutionary methods are methods based on evolutionary algorithms such as genetic algorithm[39] and particle swarm optimization algorithm[40, 41]. The weighted sum method [42], which is simple and readily applicable to engineering practice, is adopted in this study to formulate a compound single-objective optimization problem as shown in Eq. (13). The compound single objective function is mathematically expressed as a sum of weighted individual objective functions. The weightings can

be assigned by the users. Considering different objective functions may have different magnitudes, the individual objective function (J_{cost}, $J_{comfort}$ and $J_{peak,DR}$) is normalized by its own optimal value (J^*_{cost} , $J^*_{comfort}$ and $J^*_{peak,DR}$). After the normalization, all dimensionless objective functions are multiplied with corresponding weightings, i.e. thermal comfort weighting α, peak power weighting β, and cost weighting (1- α - β). Given a set of indoor air temperature set-point schedule $\{T_{set,1}, T_{set,2}, \ldots, T_{set,k}\}$, the indoor air temperature and power consumption can be predicted using the integrated thermal models. Note that due to the nonlinear characteristics of dynamics of the integrated thermal response models, the optimization problem is a nonlinear programming problem and an advanced optimization solver is needed to search the optimal schedule of the indoor air temperature set-points.

$$\min_{\{T_{set,1},T_{set,2},\ldots,T_{set,k}\}}((1-\alpha-\beta)\frac{J_{cost}}{J^*_{cost}}+\alpha\frac{J_{comfort}}{J^*_{comfort}}+\beta\frac{J_{peak,DR}}{J^*_{peak,DR}}) \tag{13}$$

$$J_{cost}=\sum_{i=1}^{m}E_iC_i; \tag{13-a}$$

$$J_{comfort}=\sqrt{\frac{1}{n}\sum_{j=1}^{n}(T_{in,j}-T_{in,exp,j})^2}; \tag{13-b}$$

$$J_{peak,DR}=max\{P_1,P_2,\ldots,P_l\}; \tag{13-c}$$

Subject to $$T_{set.lb}\le T_{set,k}\le T_{set,ub} \tag{14}$$

where $J^*_{cost}=min\{J_{cost}\}$; $J^*_{comfort}=min\{J_{comfort}\}$ and $J^*_{peak,DR}=min\{J_{peak,DR}\}$.

3.3. GA-based optimization

Conventional optimization techniques depend strongly on the initial values and are apt to get a local optimization. GA is an evolutionary search algorithm inspired by the process of natural selection. It makes a population of individual solutions "evolve" toward an optimal solution by successive modifications. During each modification, three main types of rules, i.e. selection, crossover and mutation, are used to create the next generation from the current generation. GA can address a variety of optimization problems that standard gradient descent methods are incompetent to solve, such as the problems in which the objective function is discontinuous, stochastic, or highly nonlinear. GA [43, 44] has been used to solve the optimization problems in the domain of HVAC. The major reason for applying GA in this study is that the algorithm is gradient free and the target problem is a nonlinear

programming problem. Population-Size, Max-Generations and Function-Tolerance are three important parameters in the GA optimization, which indicate the number of individuals in each generation, the maximum number of iterations before the algorithm halts and the termination tolerance, respectively. In this study, they are assigned with the values of 100, 160 and 1×10^{-6}, respectively. The GA optimization is solved by using MATLAB on a desktop computer with Intel Core i7-4790 (3.60 GHz), 16 GB of memory, under Windows 10 64-bit operating system. The runtime of the GA optimization in our case study is around 80 minutes. As the model-based DR control method for residential inverter ACs developed in this study is to respond to day-ahead electricity pricing which is forecasted by the utility or third-party load aggregator and delivered to the end-users one day ahead, the runtime is acceptable.

4. Results and discussions

4.1. Test conditions

Dynamic electricity pricing is one of the key components in the implementation of DR programs. DAP and RTP are the most commonly used dynamic electricity pricings used by Independent System Operators (ISO) or Regional Transmission Operators (RTO) such as Electricity Reliability Council of Texas (ERCOT), PJM or New York ISO. Fig. 7 shows the historical DAP data of the PJM energy market from June to July 2016 [45]. The average DAP profile is used for case studies. Weather forecast data from local observatory, pre-defined occupancy profiles and day-ahead electricity prices from electric utilities are used as the inputs.

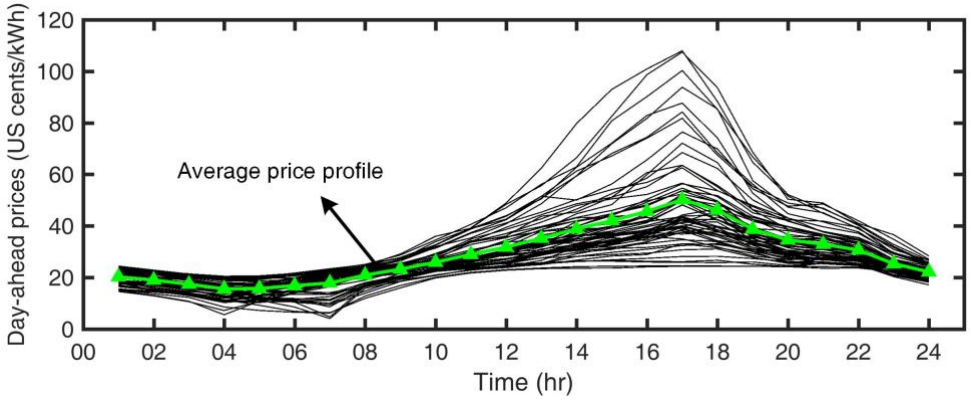

Fig. 7. Day-ahead pricing data of the PJM energy market from June to July 2016.

Case studies in this study are carried out on a typical hot summer day. Fig. 8 shows the outdoor weather conditions and internal heat gains from 8:00 to 8:00 on the next day. The room is unoccupied from 8:00 to 18:00 considering the occupants are out for school or work during day time. Signals of DR events, which normally last for 2 to 4 hours, are determined and delivered by the electric utilities. The DR event here is assumed to start at 16:00 to end at 20:00, which is the typical time period when the residential buildings are occupied and the regional electricity consumption is high. The simulation starts from 8:00 in the morning. It is assumed that the room thermal response is stabilized after one-night AC operation and control, therefore, the AC temperature set-point is used as the initial value of indoor air temperature in the simulation. The time step for simulation is set as 1 minute.

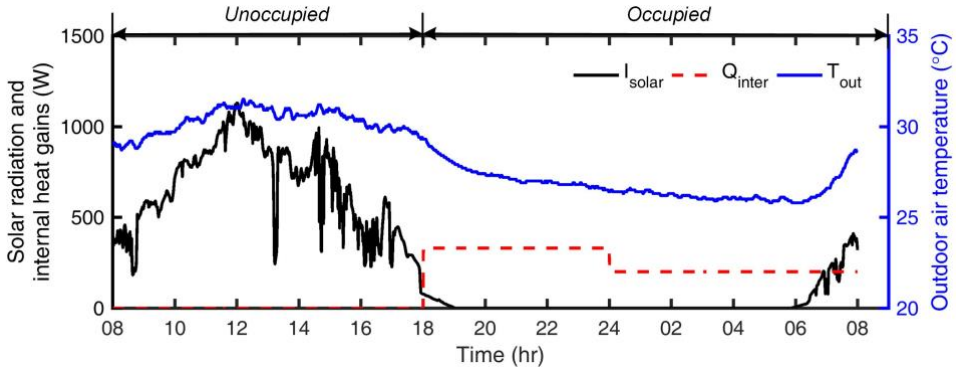

Fig. 8. Outdoor weather conditions and internal heat gains on a typical hot summer day.

4.2. Baseline case without DR control

A baseline case without DR is tested for comparison purpose. The indoor air temperature set-point from 18:00 to 08:00 on the next day is fixed as 24°C in the baseline case. The PID controller parameters are tuned manually in this study with K_p = 5, K_i = 1 and K_d = 5. Average hourly power consumption, hourly electricity cost and indoor air temperature are shown in Fig. 9 - Fig. 10 for comparisons with the GA-based cases.

4.3. GA-based cases

Different from the baseline case, the pre-cooling strategy is adopted in the GA-based cases which means the AC is allowed to be turned on from 16:00 to 18:00 before the room is occupied. The energy consumptions and electricity costs from 16:00 to 08:00 on the next day are also taken into account when calculating the objective function of Eq. (13-a), i.e. m = 16 hours. The temperature deviations are considered only when the room is occupied, i.e. 18:00 to 8:00 on the next day and n = 840 minutes

in Eq. (13-b). The peak power demand during DR hours in Eq. (13-c) is the maximum value of power from 16:00 to 20:00, i.e. l = 240 minutes. To satisfy the thermal comfort of occupants, the temperature set-points are searched in the range of 22℃ - 26℃ with a constant interval of 0.5 ℃.

The optimal temperature set-point schedule searched by the GA-based method is affected by both thermal comfort weighting α and peak power weighting β. Three groups of cases are tested for investigating the impacts of the weightings on the optimization results. In each group of cases (e.g., Case 1), the peak power weightings are 0.3, 0.4 and 0.5 respectively (i.e., Case 1-a, 1-b and 1-c) while the thermal comfort weightings are the same. Different groups of cases adopt different thermal comfort weightings, i.e. 0.2 for Case 1, 0.3 for Case 2 and 0.5 for Case 3. Table 2 shows the whole-day indoor air temperature set-point schedules in the baseline case and GA-based cases. The schedules in the GA-based cases are the optimized results. Table 3 compares the performances of the GA-based cases with the baseline case in terms of peak power reductions, electricity cost savings and temperature deviations. Mean absolute error (MAE) and root mean square error (RMSE) are used to quantify the temperature deviations from the temperature set-points. Some common features in all GA Cases can be found as follows. Compared with the baseline case, the peak power consumptions and total electricity costs in all GA-based cases have certain reductions. In terms of thermal comfort, the indoor air temperatures in the GA-based cases have larger temperature deviations, but they still remain in the comfort constraint of 22℃ - 26℃.

Table 2. Indoor air temperature set-point schedules in baseline case and GA-based cases

Time of day		Indoor air temperature set-point schedules (℃)									
Start	End	Baseline Case	GA Cases								
			Case 1-a	Case 1-b	Case 1-c	Case 2-a	Case 2-b	Case 2-c	Case 3-a	Case 3-b	Case 3-c
08:00	16:00	off	off	off	off	off	off	off	off	off	off
16:00	17:00	off	25.5	26	26	25.5	25.5	26	25.5	25.5	26
17:00	18:00	off	25.5	26	26	25.5	25.5	26	25.5	25.5	25.5
18:00	19:00	24	25.5	26	26	25	25	25.5	24.5	25	25
19:00	20:00	24	25	26	26	24.5	25	25.5	24.5	24.5	24.5
20:00	21:00	24	24.5	23	25	24	24	25	24.5	24	24
21:00	22:00	24	24	25	26	24	24.5	24.5	24	24	24
22:00	23:00	24	24	25	26	24	24	24.5	24.5	24.5	24
23:00	00:00	24	25	25	24	25	25	24.5	24	24	24.5
0:00	01:00	24	24.5	25	25.5	24.5	24	24.5	24	24	24
01:00	02:00	24	24.5	24.5	25	24.5	24	23.5	24	24	24
02:00	03:00	24	24.5	24.5	25	24	23.5	25	24	24	24.5

03:00	04:00	24	25.5	23.5	25.5	24	24	24.5	24.5	24	23.5
04:00	05:00	24	25.5	23.5	25	24	24	24.5	25	24.5	23.5
05:00	06:00	24	25	26	26	23.5	24	24	24.5	23.5	24.5
06:00	07:00	24	23.5	24	24.5	23.5	25	25	24	24	23.5
07:00	08:00	24	26	25	25	25	24	25	24.5	25	24.5

Table 3. Performance comparison in baseline case and GA-based cases

Cases	Comfort weighting	Peak weighting	Peak power demand during DR hours (W)	Peak power reduction (%)	Electricity cost (Cents)	Cost saving (%)	Temperature deviation (℃)	
							MAE	RMSE
Baseline Case			1343.0	0	161.98	0	0.05	0.37
GA Case 1-a	0.2	0.3	566.2	57.84%	131.43	18.86%	0.50	0.65
GA Case 1-b	0.2	0.4	444.9	66.87%	133.47	17.60%	0.79	0.99
GA Case 1-c	0.2	0.5	444.9	66.87%	101.22	37.51%	1.01	1.19
GA Case 2-a	0.3	0.3	566.2	57.84%	142.22	12.20%	0.34	0.48
GA Case 2-b	0.3	0.4	566.2	57.84%	139.92	13.62%	0.31	0.50
GA Case 2-c	0.3	0.5	444.9	66.87%	121.97	24.70%	0.57	0.73
GA Case 3-a	0.5	0.3	702.6	47.68%	145.17	10.37%	0.20	0.29
GA Case 3-b	0.5	0.4	566.2	57.84%	144.66	10.69%	0.22	0.36
GA Case 3-c	0.5	0.5	549.4	59.09%	143.98	11.11%	0.31	0.43

4.3.1. Sensitivity analysis of peak power weighting

Three sets of GA-based cases (i.e. Case 1, 2 and 3) are studied to investigate the sensitivity of the optimization method to the peak power weighting. In each set of cases, the thermal comfort weightings remain fixed as 0.2, 0.3 and 0.5, respectively, and the peak power weightings are set as 0.3, 0.4 and 0.5 in each set. Average hourly power consumption, electricity cost and indoor air temperature in all cases are shown in Fig 9. It can be found that when the thermal comfort weighting is fixed, peak power consumptions during DR hours and total electricity costs decrease with the increase of the peak power weighting. This is because the increase of the peak power weighting means the peak power reduction is considered to be more important in searching the optimal solution using GA. As shown in Table 3, the maximum peak power reductions are achieved with the largest peak power weightings in each set of GA-based cases, i.e. 66.87% in Case 1-c, 66.87% in Case 2-c and 59.09% in Case 3-c, respectively. The minimum temperature deviations (RMSE) occur with the smallest peak power weighting in each set of GA-based cases, i.e. 0.65℃ in Case 1-a, 0.48℃ in Case 2-a, and 0.29℃ in Case 3-a, respectively. The results show that the objective function is sensitive to

the peak power weighting, and the peak power weighting reasonably influences the optimization results to achieve the optimization purpose.

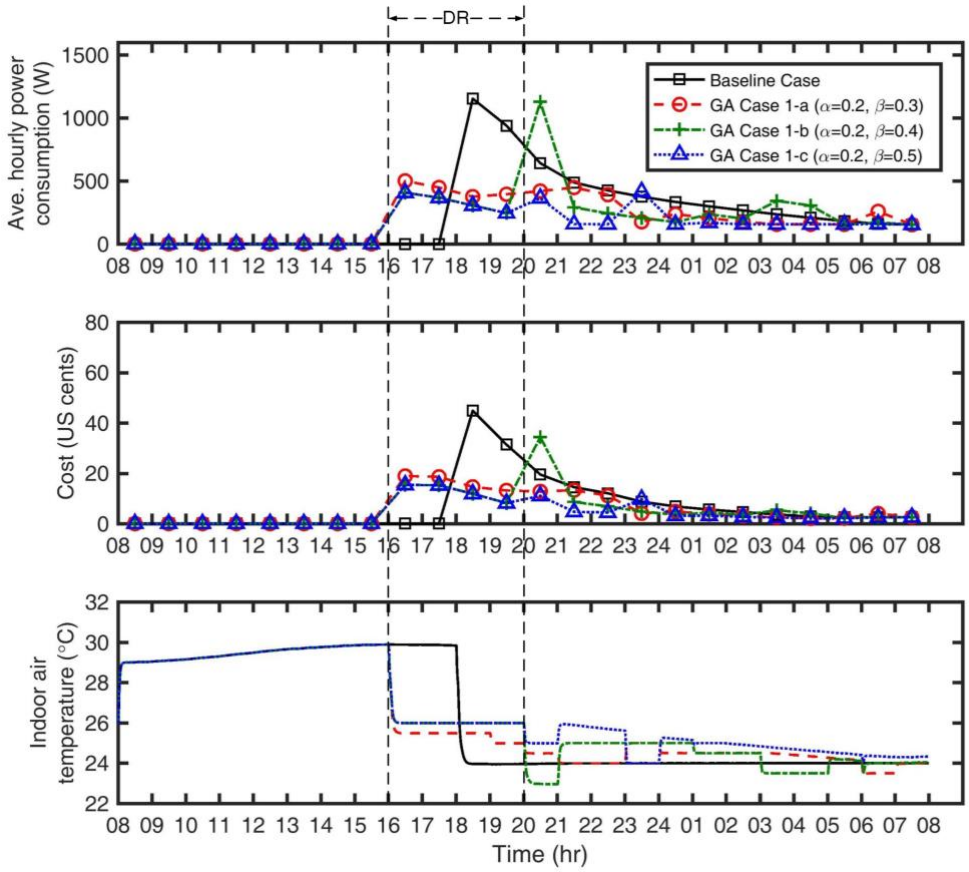

Fig. 9-a. Energy consumption, cost and indoor air temperature in the baseline case and GA-based cases ($\alpha = 0.2$, $\beta = 0.3/0.4/0.5$).

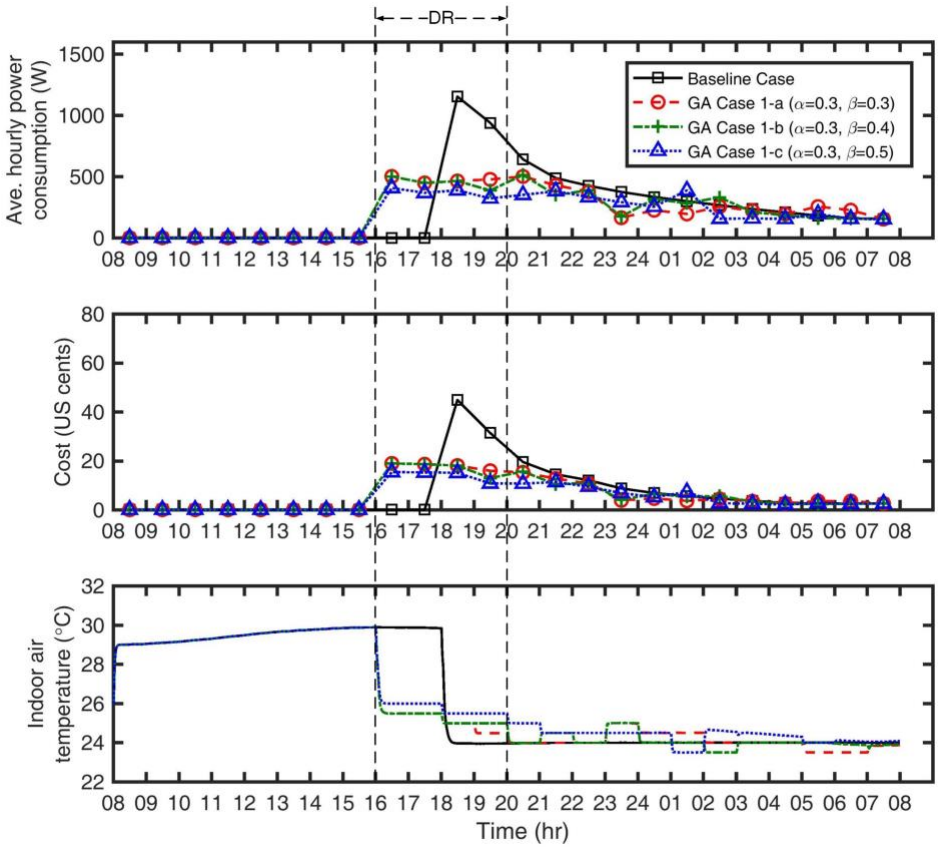

Fig. 9-b. Energy consumption, cost and indoor air temperature in the baseline case and GA-based cases (α = 0.3, β = 0.3/0.4/0.5).

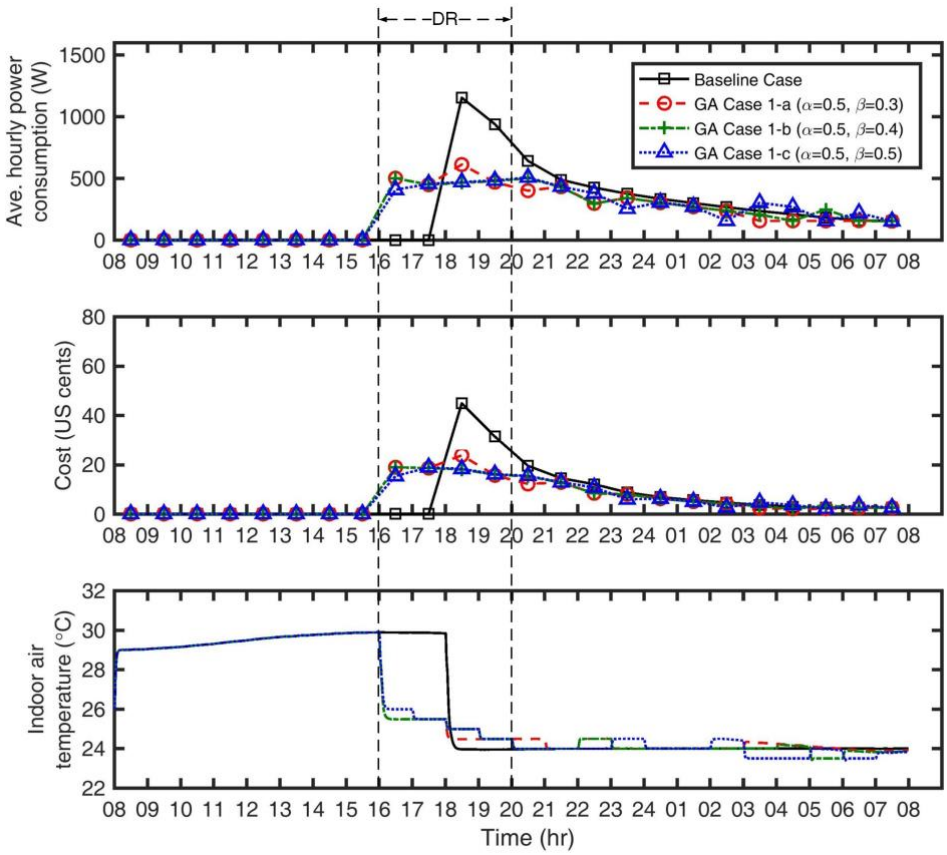

Fig. 9-c. Energy consumption, cost and indoor air temperature in the baseline case and GA-based cases ($\alpha = 0.5$, β = 0.3/0.4/0.5).

4.3.2. Sensitivity analysis of thermal comfort weighting

In order to investigate the impacts of the thermal comfort weighting on the optimization results, the simulation results are presented in a different way where the peak power weightings remain fixed at 0.3, 0.4 and 0.5 while the thermal comfort weightings are 0.2, 0.3 and 0.5 in each set of GA-based cases. Fig. 10 shows the profiles of average hourly power consumption, electricity cost and indoor air temperature in all cases. It can be seen that when the peak power weighting is fixed, peak power consumptions during DR hours and total electricity costs increase with the increase of the thermal comfort weighting. This is because the increase of the thermal comfort weighting means occupants consider maintaining thermal comfort is more important in searching the optimal solution using GA. The maximum peak power reductions are achieved with the smallest thermal comfort weighting in each set of GA-based cases, i.e. 57.84% in GA Case 1-a, 66.87% in GA Case 1-b and 66.87% in GA Case 1-c, respectively. The minimum temperature deviations (RMSE) occur with the largest thermal comfort weighting in each set of GA-based cases, i.e. 0.29℃ in GA Case 3-a, 0.36℃ in GA Case 3-b, and 0.43℃ in GA Case 3-c, respectively. The results show that the objective function is sensitive to the peak power weighting, and the peak power weighting reasonably influences the optimization results to achieve the optimization purpose.

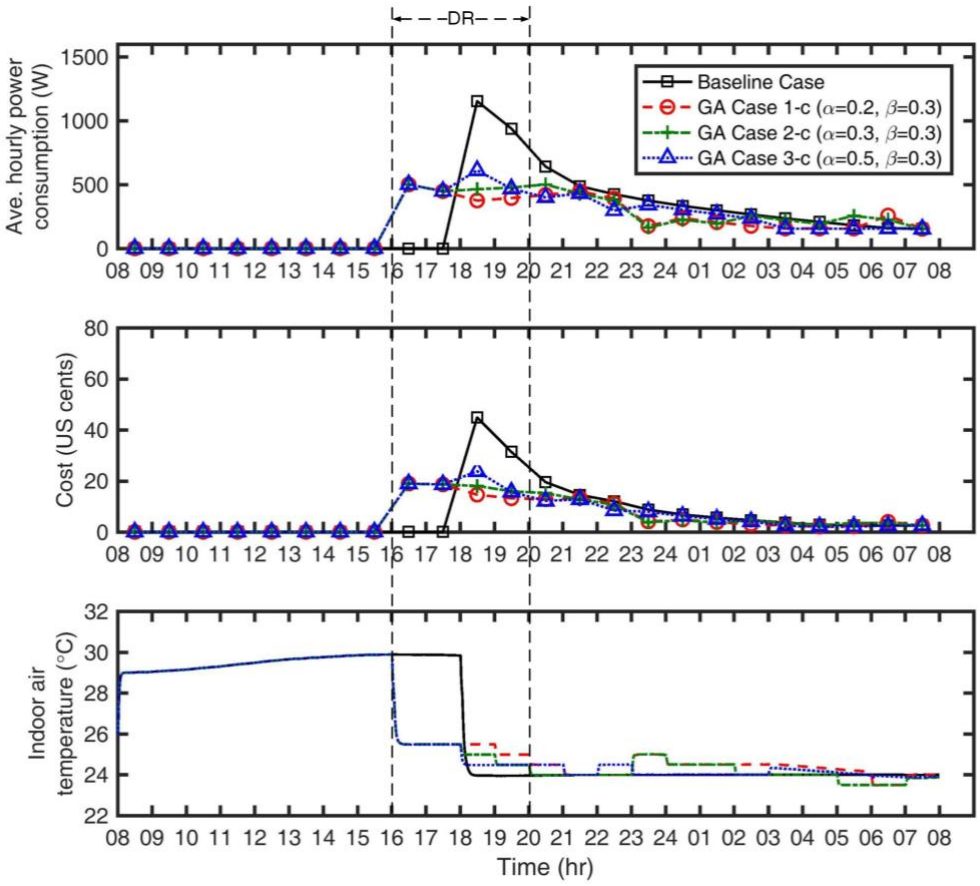

Fig. 10-a. Energy consumption, cost and indoor air temperature in the GA-based cases (α = 0.2/0.3/0.5, β = 0.3).

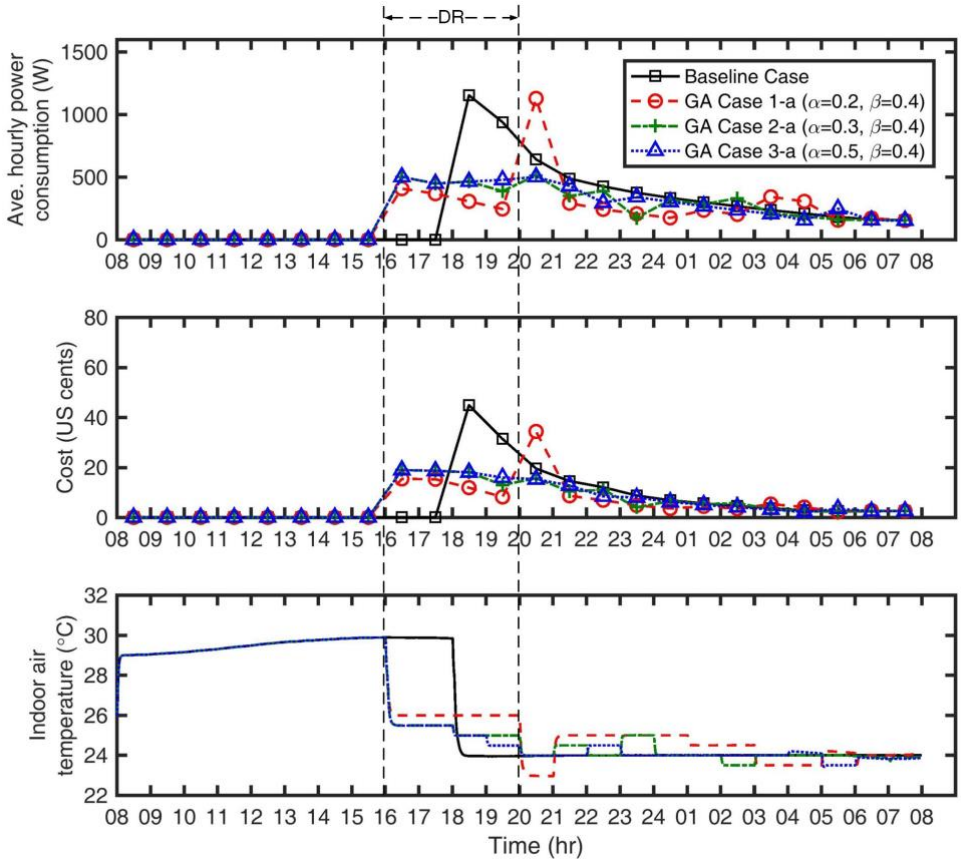

Fig. 10-b. Energy consumption, cost and indoor air temperature in the GA-based cases (α = 0.2/0.3/0.5, β = 0.4).

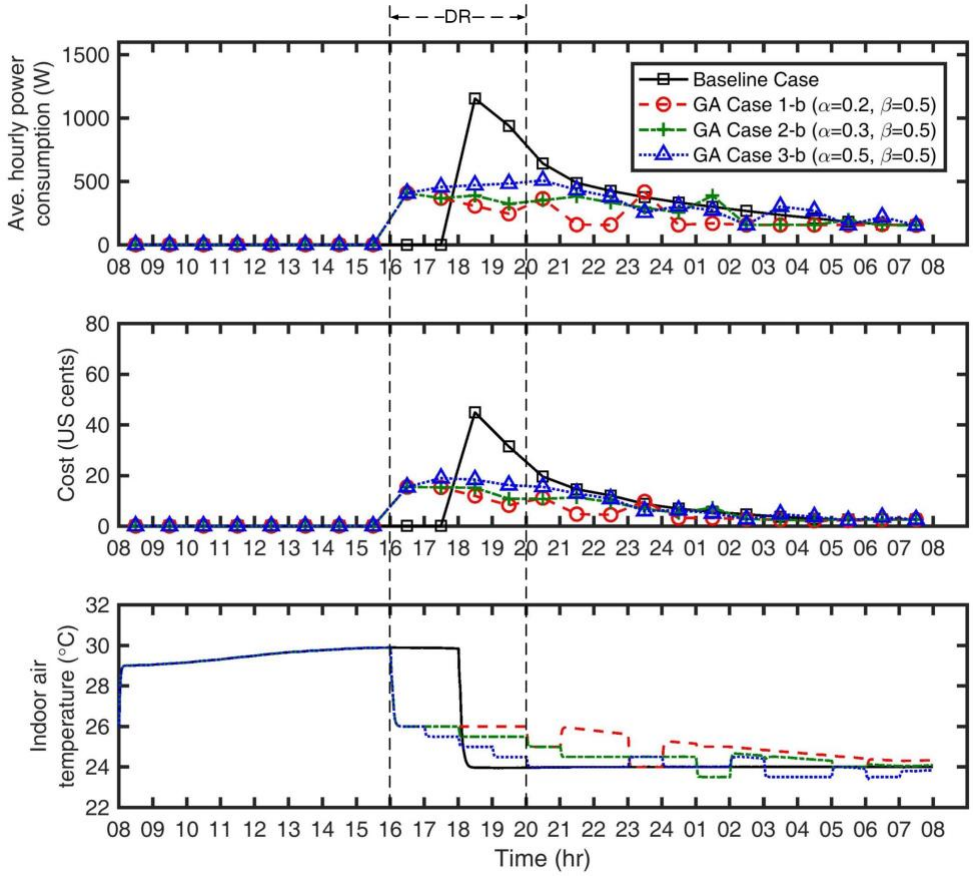

Fig. 10-c. Energy consumption, cost and indoor air temperature in the GA-based cases (α = 0.2/0.3/0.5, β = 0.5).

5. Conclusions

Dynamic electricity pricing is an effective DR program in smart grids to attract residential end-users to participate in it. It can bring about cost savings to residential homes while relieving power imbalance issue during on-peak hours. Intelligent DR control technologies for household appliances, especially ACs, are urgently required to encourage and enable wider participations. The present paper presents a model-based optimal DR control method for residential inverter ACs to achieve optimal trade-offs among electricity costs, thermal comfort and peak power reductions in the dynamic electricity pricing environment.

For the purpose of computational efficiency, control-oriented room thermal model and steady-state physical model of inverter ACs are developed and integrated for model-based control. The trade-offs among electricity costs, occupant comfort and peak power reductions during DR hours are formulated as a nonlinear programming problem with user-definable weightings. GA, as an advanced and

effective optimization method, is used to solve the optimization problems. Simulation results show that the proposed model-based optimal control method can reduce the peak power consumptions of inverter ACs and reduce the electricity costs while still satisfying the thermal comfort constraints. Sensitivity analyses of the weightings in the normalized objective function show that the objective function is reasonably formulated, which sensitive to both peak power weighting and thermal comfort weighting. Minimizing the comprehensive objective function can effectively achieve the optimal trade-offs among the electricity costs, occupant comfort and peak power reductions. The proposed model-based optimal control method can be implemented in the smart HEMSs and enable the residential inverter ACs to automatically respond to the day-ahead dynamic electricity prices to achieve the optimal trade-offs. When a large number of residential ACs simultaneously respond to dynamic electricity prices from utilities or third-party load aggregators, power consumptions in grid during on-peak hours can be significantly reduced. In our future work, we will develop a simplified inverter AC model for real-time control and develop automatic DR control method to respond to real-time dynamic prices.

Acknowledgement

The research work presented in this paper is financially supported by a research grant (G-YBTB) in the Hong Kong Polytechnic University (PolyU) and the Strategic Focus Area (SFA) Scheme (1-BBW7) of Research Institute for Sustainable Urban Development (RISUD) in PolyU. The support is gratefully acknowledged.

Appendix A. Effectiveness-NTU (ε-NTU) method and heat transfer correlations

In the ε-NTU method, the actual heat transfer between the refrigerant and air for each zone can be calculated by Eqs. (A.1) - (A.11).

$$C_{ref} = \dot{m}_{ref} c_{ref} \tag{A.1}$$

$$C_{air} = \dot{m}_{air} c_{air} \tag{A.2}$$

$$C_{min} = \min(C_{ref}, C_{air}) \tag{A.3}$$

$$C_{max} = \max(C_{ref}, C_{air}) \tag{A.4}$$

$$c_r = \frac{C_{min}}{C_{max}} \quad \text{(A.5)}$$

$$A_{sur} = \pi D_o L \quad \text{(A.6)}$$

$$U_{ov} = 1/(\frac{1}{\alpha_{ref}} + \frac{1}{2}\frac{D_o}{\lambda_w} ln\frac{D_o}{D_i} + \frac{1}{r\alpha_{air}}) \quad \text{(A.7)}$$

$$NTU = U_{ov}A_{sur}/C_{min} \quad \text{(A.8)}$$

$$\varepsilon = (1 - e^{-NTU(1-c_r)})/(1 - c_r e^{-NTU(1-c_r)}) \quad \text{(A.9)}$$

$$Q_{max} = C_{min}|T_{ref,in} - T_{air,in}| \quad \text{(A.10)}$$

$$Q_{ref,air} = \varepsilon Q_{max} \quad \text{(A.11)}$$

where C_{ref} and C_{air} are the refrigerant and air thermal capacitance rates, W/K; U_{ov} is the tube overall heat transfer coefficient from the refrigerant side to the air side, W/(m^2•K); *NTU* is the number of transfer unit; ε is the heat transfer effectiveness; α_{ref} and α_{air} are the heat transfer coefficients at the refrigerant and air sides, W/(m^2•K). The heat transfer coefficients (HTCs) are critical parameters in the heat exchanger modeling. For different zones in the heat exchangers, the correlations used for calculating HTCs at the refrigerant and air sides are different, as shown in Table A1.

Table A1. Correlations for the calculations of heat transfer coefficients.

Regions		Correlations for HTCs	
		Refrigerant side	Air side
Condenser	De-superheated zone	Petukhov correlation [46]	Wang et al. [47] (Dry condition)
	Two-phase zone	Cavallini correlation [48]	
	Subcooled zone	Gnielinski correlation [49]	
Evaporator	Two-phase zone	Kandlikar correlation [50]	
	Superheated zone	Petukhov correlation [46]	Wang et al. [51] (Wet condition)

References

[1] Somasundaram S, Pratt R, Akyol B, Fernandez N, Foster N, Katipamula S, et al. Reference guide for a transaction-based building controls framework. Pacific Northwest National Laboratory. 2014.

[2] Electrical and Mechanical Services Department. Hong Kong Energy End-use Data 2017. Hong Kong2017.

[3] Commission CE. California Energy Demand: 2000-2010. California Energy Commission, Sacramento. 2000.

[4] Xu P, Haves P. Case study of demand shifting with thermal mass in two large commercial buildings. ASHRAE Transactions. 2006;112:572.

[5] Yin R, Xu P, Piette MA, Kiliccote S. Study on Auto-DR and pre-cooling of commercial buildings with thermal mass in California. Energy and Buildings. 2010;42:967-75.

[6] Ruan Y, Liu Q, Li Z, Wu J. Optimization and analysis of Building Combined Cooling, Heating and Power (BCHP) plants with chilled ice thermal storage system. Applied Energy. 2016;179:738-54.

[7] Patteeuw D, Bruninx K, Arteconi A, Delarue E, D'haeseleer W, Helsen L. Integrated modeling of active demand response with electric heating systems coupled to thermal energy storage systems. Applied Energy. 2015;151:306-19.

[8] Cui B, Gao D-c, Wang S, Xue X. Effectiveness and life-cycle cost-benefit analysis of active cold storages for building demand management for smart grid applications. Applied Energy. 2015;147:523-35.

[9] Federal Energy Regulatory Commission. Assessment of demand response and advanced metering. 2014.

[10] Zhou B, Li W, Chan KW, Cao Y, Kuang Y, Liu X, et al. Smart home energy management systems: Concept, configurations, and scheduling strategies. Renewable and Sustainable Energy Reviews. 2016;61:30-40.

[11] Chen Z, Wu L, Fu Y. Real-time price-based demand response management for residential appliances via stochastic optimization and robust optimization. Smart grid, IEEE transactions on. 2012;3:1822-31.

[12] Hubert T, Grijalva S. Modeling for residential electricity optimization in dynamic pricing environments. Smart Grid, IEEE Transactions on. 2012;3:2224-31.

[13] Lujano-Rojas JM, Monteiro C, Dufo-López R, Bernal-Agustín JL. Optimum residential load management strategy for real time pricing (RTP) demand response programs. Energy Policy. 2012;45:671-9.

[14] Thomas AG, Jahangiri P, Wu D, Cai C, Zhao H, Aliprantis DC, et al. Intelligent residential air-conditioning system with smart-grid functionality. Smart Grid, IEEE Transactions on. 2012;3:2240-51.

[15] Li S, Zhang D, Roget AB, O'Neill Z. Integrating home energy simulation and dynamic electricity price for demand response study. Smart Grid, IEEE Transactions on. 2014;5:779-88.

[16] Yoon JH, Bladick R, Novoselac A. Demand response for residential buildings based on dynamic price of electricity. Energy and Buildings. 2014;80:531-41.

[17] Aswani A, Master N, Taneja J, Culler D, Tomlin C. Reducing transient and steady state electricity consumption in HVAC using learning-based model-predictive control. Proceedings of the IEEE. 2012;100:240-53.

[18] Qureshi T, Tassou S. Variable-speed capacity control in refrigeration systems. Applied Thermal Engineering. 1996;16:103-13.

[19] Henze GP, Felsmann C, Knabe G. Evaluation of optimal control for active and passive building thermal storage. International Journal of Thermal Sciences. 2004;43:173-83.

[20] Ma Y, Kelman A, Daly A, Borrelli F. Predictive control for energy efficient buildings with thermal storage. IEEE Control System Magazine. 2012;32:44-64.

[21] Hu M, Xiao F, Wang L. Investigation of demand response potentials of residential air conditioners in smart grids using grey-box room thermal model. Applied Energy. 2017;207:324-35.

[22] Hu M, Xiao F. Investigation of the Demand Response Potentials of Residential Air Conditioners Using Grey-box Room Thermal Model. Energy Procedia. 2017;105:2759-65.

[23] Hu M, Xiao F, Wang L. Investigation of demand response potentials of residential air conditioners in smart grids using grey-box room thermal model. Applied Energy. 2017.

[24] He X-D, Liu S, Asada HH. Modeling of Vapor Compression Cycles for Multivariable Feedback Control of HVAC Systems. Journal of Dynamic Systems, Measurement, and Control. 1997;119:183-91.

[25] Rasmussen BP. Dynamic modeling and advanced control of air conditioning and refrigeration systems: UIUC; 2005.

[26] Koury R, Machado L, Ismail K. Numerical simulation of a variable speed refrigeration system. International journal of refrigeration. 2001;24:192-200.

[27] Kapadia R, Jain S, Agarwal R. Transient characteristics of split air-conditioning systems using R-22 and R-410A as refrigerants. HVAC&R Research. 2009;15:617-49.

[28] Leducq D, Guilpart J, Trystram G. Low order dynamic model of a vapor compression cycle for process control design. Journal of food process engineering. 2003;26:67-91.

[29] Zhou R, Zhang T, Catano J, Wen JT, Michna GJ, Peles Y, et al. The steady-state modeling and optimization of a refrigeration system for high heat flux removal. Applied Thermal Engineering. 2010;30:2347-56.

[30] Choi JM, Kim YC. Capacity modulation of an inverter-driven multi-air conditioner using electronic expansion valves. Energy. 2003;28:141-55.

[31] Grald EW, MacArthur JW. A moving-boundary formulation for modeling time-dependent two-phase flows. International Journal of Heat and Fluid Flow. 1992;13:266-72.

[32] He X-D, Liu S, Asada HH, Itoh H. Multivariable control of vapor compression systems. HVAC&R Research. 1998;4:205-30.

[33] Rasmussen BP, Alleyne AG. Control-Oriented Modeling of Transcritical Vapor Compression Systems. Journal of Dynamic Systems, Measurement, and Control. 2004;126:54-64.

[34] Zakula T, Gayeski NT, Armstrong PR, Norford LK. Variable-speed heat pump model for a wide range of cooling conditions and loads. HVAC&R research. 2011;17:670-91.

[35] Meissner JW, Abadie MO, Moura LM, Mendonça KC, Mendes N. Performance curves of room air conditioners for building energy simulation tools. Applied Energy. 2014;129:243-52.

[36] Cherem-Pereira G, Mendes N. Empirical modeling of room air conditioners for building energy analysis. Energy and Buildings. 2012;47:19-26.

[37] Gayeski NT. Predictive pre-cooling control for low lift radiant cooling using building thermal mass: Massachusetts Institute of Technology; 2010.

[38] Zhou Q, Wang S, Xu X, Xiao F. A grey-box model of next-day building thermal load prediction for energy-efficient control. International Journal of Energy Research. 2008;32:1418-31.

[39] Deb K, Pratap A, Agarwal S, Meyarivan T. A fast and elitist multiobjective genetic algorithm: NSGA-II. IEEE transactions on evolutionary computation. 2002;6:182-97.

[40] Baghaee HR, Mirsalim M, Gharehpetian GB, Kaviani AK. Security/cost-based optimal allocation of multi-type FACTS devices using multi-objective particle swarm optimization. Simulation. 2012;88:999-1010.

[41] Baghaee HR, Mirsalim M, Gharehpetian GB, Talebi HA. Reliability/cost-based multi-objective Pareto optimal design of stand-alone wind/PV/FC generation microgrid system. Energy. 2016;115:1022-41.

[42] Grodzevich O, Romanko O. Normalization and other topics in multi-objective optimization. Proceedings of the Fields–MITACS Industrial Problems Workshop2006.

[43] Wang S, Xu X. Parameter estimation of internal thermal mass of building dynamic models using genetic algorithm. Energy Conversion and Management. 2006;47:1927-41.

[44] Tuhus-Dubrow D, Krarti M. Genetic-algorithm based approach to optimize building envelope design for residential buildings. Building and Environment. 2010;45:1574-81.

[45] PJM Interconnection. Hourly Real-Time & Day-Ahead Locational Marginal Pricing. Available from: http://www.pjm.com/markets-and-operations/energy/real-time/monthlylmp.aspx.

[46] Petukhov B. Heat transfer and friction in turbulent pipe flow with variable physical properties. Advances in heat transfer. 1970;6:503-64.

[47] Wang C-C, Lee C-J, Chang C-T, Lin S-P. Heat transfer and friction correlation for compact louvered fin-and-tube heat exchangers. International journal of heat and mass transfer. 1999;42:1945-56.

[48] Cavallini A, Col DD, Doretti L, Matkovic M, Rossetto L, Zilio C, et al. Condensation in horizontal smooth tubes: a new heat transfer model for heat exchanger design. Heat Transfer Engineering. 2006;27:31-8.

[49] Gnielinski V. New equations for heat and mass-transfer in turbulent pipe and channel flow. International chemical engineering. 1976;16:359-68.

[50] Kandlikar SG. A general correlation for saturated two-phase flow boiling heat transfer inside horizontal and vertical tubes. Journal of heat transfer. 1990;112:219-28.

[51] Wang C-C, Lin Y-T, Lee C-J. Heat and momentum transfer for compact louvered fin-and-tube heat exchangers in wet conditions. International journal of heat and mass transfer. 2000;43:3443-52.